Biological Evaluation of Copper Based Drug as Chemotherapeutic Agent with tRNA

Waddhaah M. Al–Asbahy[1], Niyazi A. S. Al-Areqi[1], Gamal Al-amery[2], Manal Shamsi[1], Hadeel Sami Mukbil[3,*]

Abstract— The interaction of new dinuclear copper(II) complex 1, $[Cu_2(glygly)_2(ppz)(H_2O)_4].{}_2H_2O$, derived from dipeptide (glycyl glycine anion) and piperazine as a metallopeptide drug with tRNA was examined by UV–visible, Fourier transform- infrared (FT–IR), and fluorescence spectroscopy, circular dichroism (CD), and isothermal titration calorimetry (ITC). The binding constants (K_b), and binding site number (n), and corresponding thermodynamic parameters; ΔG, ΔH and ΔS were calculated. ITC results showed that the complex 1 binds strongly with tRNA ($K_b \sim 4.504 \times 10^4\ M^{-1}$). The distance between tRNA (donor) and complex 1 (acceptor) was estimated by means of fluorescence resonance energy transfer (FRET). The molecular docking technique utilized for ascertaining the mechanism and mode of action towards the molecular target tRNA indicated that complex 1 has a strong binding affinity to tRNA. Moreover, the growth inhibitory effects of the complex 1 on the SW480 cancer cell line were measured (IC50 ~ 2.87 µg/ml).

Index Terms—transfer RNA; *In vitro* tRNA binding; Circular dichroism; Thermal denaturation; Fluorescence spectroscopy.

1 Introduction

COPPER (II) complexes are considered as the most promising alternatives to cisplatin as anticancer drugs. Serum copper levels correlate with tumor incidence and weight, malignant progression, and recurrence in a variety of human cancers; namely Hodgkin's lymphoma, sarcoma, leukemia, and cancer of cervix, breast, liver, and lung as well as brain tumors [1, 2]. Interestingly, the high serum and tissue levels of copper, found in many types of human cancers, support the idea that copper could be used as a potential tumor–specific target [3]. The research design of binding small metal based drug molecules with tRNA at physiological conditions is of a great interest for the biological processes and the development of novel therapeutic agents. Ribonucleic acid (RNA) has been offered several advantages as attractive target for therapeutic intervention in drug discovery in comparison to DNA due to its unique three dimensional (3D) pockets for specific binding for small ligands [4]. Moreover, RNA molecules have gained remarkable prominence due to the emerging knowledge of their potential and critical roles in many cellular activities and functions [5]. RNA relates to diagnosis and therapy of some diseases originated from viruses such as Human Immunodeficiency Virus (HIV), Hepatitis C Virus (HCV), influenza and flaviviruses [6]. Recently, the interaction of the drug with RNA gained major biological importance for developing RNA–targeted therapeutic agents through the understanding of structural details and thermodynamics of the binding to various RNA structures, toxic and damaging effects etc [7,8].

These studies provide an important rationale for design of new lead anticancer drugs at the active site of action, besides providing the pharmacological profile *in vitro*. Complex 1 – a dinuclear copper(II) dipeptide piperazine bridged scaffold (Fig. 1) fulfills all the pre–requirements of an efficient chemotherapeutic agent owing to (i) its good aqueous solubility which facilitates its rapid cellular uptake, (ii) high DNA binding propensity also revealed by molecular docking, (iii) high cytotoxic activity, thereby capable of inhibition of DNA synthesis of cancerous cells specifically *via* apoptotic pathways, (iv) specific binding domain for selective recognition and cleavage, (v) unique peptide and piperazine scaffold (recognition element domain) with asymmetric binuclear copper centers, (vi) intramolecular H– bond forming molecular topology [9]. One approach to the development of RNA targeted drug molecules has been to study the interaction of well rely on a deeper understandingof these binding processes. Therefore, it was thought worthwhile to carry out studies of complex 1 with tRNA and throw insight on therapeutic efficacy of this potential cancer chemotherapeutic drug. Herein, we report the synthesis and characterization of mixed ligand dinuclear copper(II) complex derived from piperazine and dipeptide (glycyl glycine anion) ligand scaffold as potential chemo–therapeutic drug candidates. The interaction between complex 1 and tRNA was investigated by various spectroscopic, spectroflorimetric, thermal melting experiments, and molecular docking methods. The results were supplemented with thermodynamic studies utilizing high sensitivity isothermal titration calorimetry.

- [1]*Department of Chemistry, Faculty of Applied Science, Taiz University, Taiz, Yemen.Corresponding Author E-mail: Wadahm2007@yahoo.com*
- [2]*Department of Medical Microbiology, Faculty of Medicine & Health Sciences, Taiz University, Taiz, Yemen.*
- [3]*Department of Pharmacy, Faculty of Medicine & Health Sciences, Taiz University, Taiz, Yemen. Corresponding Author E-mail: hadeelalabsi39@gmail.com*

2 Materials & Methods

2.1 Apparatus and reagents

Yeast tRNA (Type IX from Torula yeast) was purchased from Sigma–Aldrich Corporation and was stored at 4 ˚C. Its concentration was determined spectrophotometrically using a molar

extinction coefficient (ε ~ 6900 $M^{-1}cm^{-1}$ at 260 nm) expressed in terms of nucleotide phosphates [10]. Tris(hydroxymethyl) aminomethane or Tris buffer from Sigma were used as received. Doubly distilled water was used as the solvent throughout the experiments.

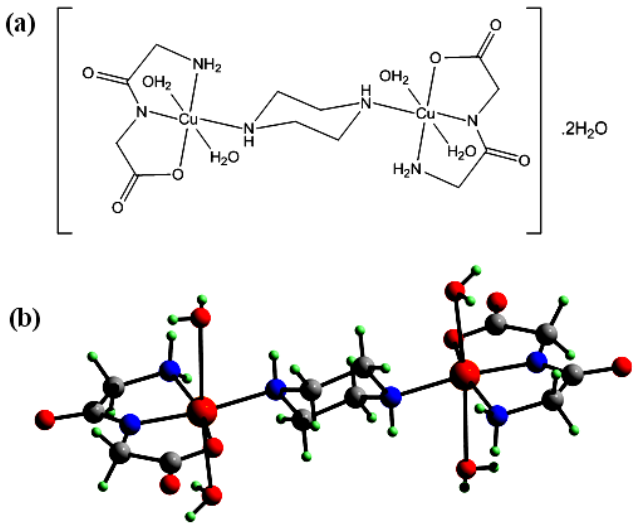

Fig.1. (a) Chemical structure and (b) ball and stick model of complex 1, $[Cu_2(glygly)_2(ppz)(H_2O)_4].2H_2O$.

Stock solution of the complex (1×10^3 M) was prepared by dissolving the complex in doubly distilled water. NaCl (analytical grade, 1 M) solution was used to maintain the ionic strength of buffer at 0.1 M, pH was adjusted to 7.4 by using HCl. Working standard solution was obtained by appropriate dilution of the stock solution. All reagents were of the best commercial grade and were used without further purification.

Electronic spectra were recorded on UV–1700 PharmaSpec UV–vis spectrophotometer (Shimadzu). Data were reported in $\lambda_{max/nm}$. Interaction of the complex with tRNA was performed in 0.01 M buffer (pH 7.4). Solutions of RNA in buffer gave a ratio of absorbance at 260 nm and 280 nm of indicating that the sample was free from protein contaminations.

Fluorescence measurements were carried out on a spectrofluorimeter (Hitachi F–2500, Tokyo, Japan) equipped with a 150 W Xenon lamp source and a 1 cm path–length quartz cell.

Circular dichroism (CD) spectra were measured on Jasco J–815–CD spectropolarimeter at room temperature using a 1 cm quartz cuvette. Emission spectra were recorded with a Hitachi F–2500 fluorescence spectrophotometer.

2.2 *In vitro* tRNA binding studies

tRNA binding experiments include absorption spectral traces, emission spectroscopy, and CD conformed to the standard methods and practices previously adopted by our laboratory [11,12]. While measuring the absorption spectra an equal amount of tRNA was added to the compound solution and the reference solution to eliminate the absorbance of the tRNA itself, and the CD contribution by the tRNA and Tris buffer was subtracted through base line correction.

2.3 Cell culture

The SW480 cancer cells were obtained from the cell lab of Sun Yat–sen University. Both cell lines were cultured in DMEM medium supplemented with fetal bovine serum (10%), penicillin (100 units/ml), and streptomycin as antibiotics (50 units/ml) at 37 °C in CO_2 incubator (95% relative humidity, 5% CO_2).

2.4 Cell viability

Cell viability was determined by measuring the ability of cells to convert MTT dye to a purple formazan dye. For our purpose, cells were seeded in 96–well tissue culture plates at 2.5 ×103 cells/well for 24 h, and then cells were incubated with medium containing different concentrations of complex 1 for 24 h. After incubation, 20 µL/well of MTT solution (5 mg/mL PBS) was added and incubated for 4 h. The medium was aspirated and replaced with 150 µL/well DMSO to dissolve the formazan salt formed. The color intensity of the formazan solution, which reflected the cell growth condition, was measured at 570 nm using a multimode microplate reader (Tecan Infinite M200, Austria). Observation of cell morphological change was performed with an Olympus Upright fluorescence microscope (Imager Z1, Carl Zeiss).

2.5 Isothermal titration calorimetry (ITC)

Measurements were carried out with a VP–ITC titration calorimeter (MicroCal, lnc, Northampton, MA). Concentrated stock of yeast tRNA was prepared in the target buffer and diluted in the same buffer to achieve desired concentrations. In a typical experiment, complex **1** solution was placed in the calorimeter injection syringe and delivered every 3.0 min to the reaction cell containing the tRNA. Measurements were paired with control experiments for heat of mixing and dilution. Data were analyzed with Levenberg–Marquardt nonlinear regression (MicroCal ORIGINPro 8.0). The typical range of variation for enthalpy measurement was ±10%.

2.6 Molecular docking studies

The rigid molecular docking studies were performed by using HEX 6.3 software [13], is an interactive molecular graphics program for calculating and displaying feasible docking modes of RNA molecule. Structure of the complex **1** was sketched by CHEMSKETCH (http://www.acdlabs.com) and convert it into pdb format from mol format by OPENBABEL (http://www.vcclab.org/lab/babel/). The crystal structure of the RNA (PDB ID: 6TNA), was retrieved from the RCSB Protein Data Bank (http://www.rcsb.org./pdb). Visualization of the docked pose has been done by using CHIMERA

(www.cgl.ucsf.edu/chimera) and PyMol (http://pymol.sourceforge.net/) molecular graphics program.

3 Results & Discussion

The synthesis and single crystal X–ray crystallographic studies of a novel metallopeptide complex **1** of the formulation $[Cu_2(glygly)_2(ppz)(H_2O)_4].2H_2O$ (CCDC: 794697), where glygly, an anion of glycyl glycine and ppz, piperazine, were described previously [9].

3.1 Electronic absorption studies

Electronic absorption spectroscopy is an effective method to examine the binding modes of complexes with tRNA followed by the changes in the absorbance and shift in the wavelength. The interaction between the complexes and tRNA is expected to perturb the ligand centered transitions of complex. On the addition of tRNA, complex **1** shows an increase in molar absorptivity (hyperchromism; 33%) with a blue shift of 4 nm at 232–278 nm (Fig.2). These changes are typical for complexes bound to tRNA through non covalent interaction most likely by electrostatic attraction (surface binding) and could be facilitated by hydrogen–bonding interactions between coordinated –NH and $–NH_2$ with phosphate groups positioned on the edge of tRNA. Hyperchromism results from the secondary changes of tRNA double helix structure. To quantify the extent of tRNA binding, the intrinsic binding constant, K_b of the complex **1** was determined by monitoring changes in absorbance with increasing concentration of yeast tRNA given by Eq. 1, through a plot of $[tRNA]/\varepsilon_a–\varepsilon_f$ vs [tRNA], where [tRNA] represents the concentration of RNA, and ε_a, ε_f and ε_b the apparent extinction coefficient (A_{obs}/[complex **1**]), free and bound complex extinction coefficients, respectively., In plots of $[RNA]/\varepsilon_a–\varepsilon_f$ vs. [RNA], K_b is given by the ratio of slope to intercept.

$$\frac{[RNA]}{\varepsilon_a-\varepsilon_f}=\frac{[RNA]}{\varepsilon_b-\varepsilon_f}+\frac{1}{K_b(\varepsilon_a-\varepsilon_f)} \quad (1)$$

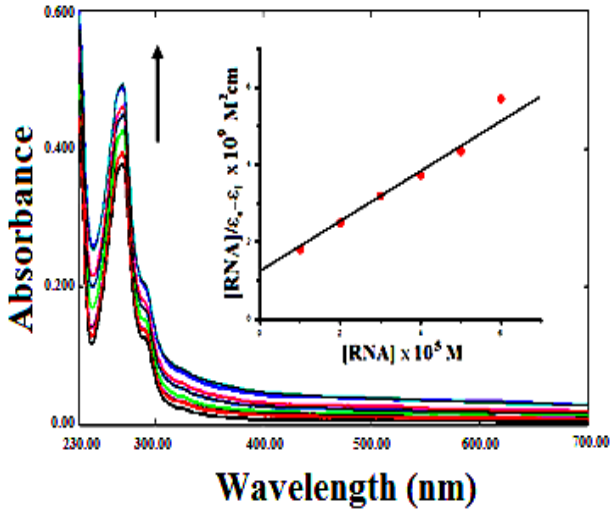

Fig. 2. Absorption spectral traces of complex **1** in 5mM Tris HCl/ 50 mM NaCl buffer at pH 7.2 upon addition of tRNA. Inset: Plots of $[tRNA]/\ \varepsilon_a–\varepsilon_f$ (M^2 cm) vs [tRNA] for the titration of tRNA with complexes ■, experimental data points; full lines, linear fitting of the data. [Complex **1**] 6.7 x 10^{-5} M, [tRNA] 0.00–3.3 x 10^{-5} M.

The intrinsic binding constant K_b values for complex **1** with tRNA were calculated and found to be 4.504×10^4 M^{-1}. Complex **1** has a strong binding affinity for tRNA for both nucleobases and phosphate [14].

3.2 Fluorescence studies (Ethidium bromide displacement assay)

Fluorescent quenching techniques is commonly used as a 'molecular ruler' in biomolecular structural studies. In the absence of tRNA, no luminescence was observed for the complex **1** in Tris–HCl buffer solution at room temperature, So, the binding of complex **1** with tRNA cannot be directly predicted through the emission spectra.

Binding experiment using ethidium bromide (EB) as a probe. EB (3,8–diamino–5–ethyl–6–phenylphenanthriumbromide), a phenanthridine fluorescence dye, is atypical probe for intercalation, form soluble complexes with tRNA and emits intense fluorescence when intercalated into the base pairs of tRNA [15]. The addition of the complexes to tRNA pretreated with EB ([tRNA]/[EB]=1) solution causes an appreciable reduction in fluorescence intensity due to replacement of EB by the complexes [16]. The complex **1** show a decrease in the emission intensity of EB–tRNA system (Fig. 3), which indicated that the complexes **1** was bind to DNA *via* electrostatic interactions releasing EB molecules gradually from the EB– tRNA system.

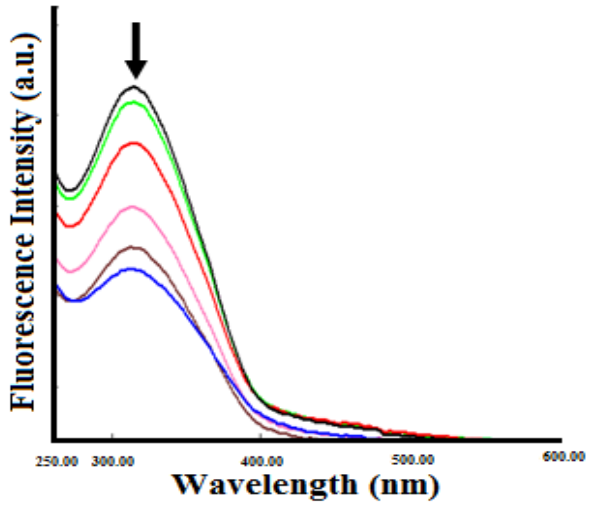

Fig.3. Emission enhancement spectra of the complex **1** in presence of tRNA. Arrow indicates the change in the intensity upon increasing tRNA

concentration.

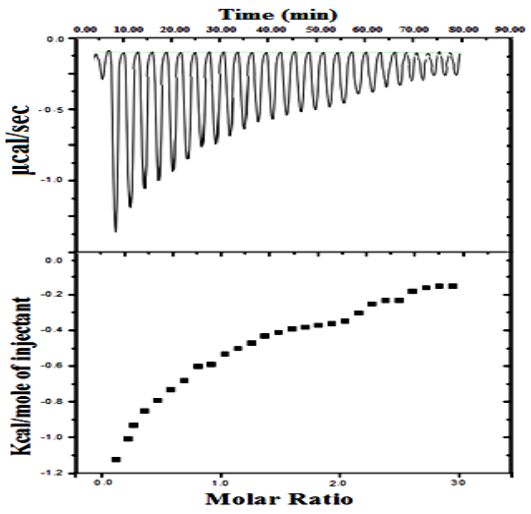

Fig.4. Isothermal titration calorimetric measurement of complex **1** with tRNA.

The quenching efficiency for each complex is evaluated by using Stern–Volmer equation [17]:

$$I_0/I = 1 + r \cdot K_{SV} \qquad (2)$$

where I_0 and I represent the fluorescence intensities in the absence and presence of the complex **1**, respectively; r is the concentration ratio of the complex to tRNA, and K_{SV} is used to evaluate the quenching efficiency and is obtained as the slope of I_0/I *vs*. r (=[complex **1**]/[tRNA]). Stern–Volmer constant, K_{SV} value for the complex **1** was found to be 2.25, indicating the strong affinity of the complex **1** to tRNA.

3.3 Isothermal titration calorimetry

ITC can give valuable information above and beyond other analytical methods, due to its ultra-sensitivity for measures the change in enthalpy (ΔH) for almost any bimolecular binding interaction [18]. To further probe the thermodynamics of the interaction of complex **1** with tRNA and dissect the observed binding free energy into enthalpic and entropic components, we have conducted ITC experiments. ITC profile for the binding of complex **1** to tRNA at 25 °C is shown in Fig. 4. Each addition of the complex **1** solution (1.0 mM) to the calorimeter cell, which contained a solution of tRNA (0.1 mM) in 0.2 mM phosphate buffer (pH =7.0) and the reference cell contained doubly distilled water, resulted in the release of heat until the binding was saturated. Upon making an injection of complex **1** heat is generated, these tiny heat effects are detected by semi–conductor thermopiles and the instrument applies thermal power (µ cal/sec) in order to actively compensate for the complex **1** induced heat effect and thus to bring the cells into thermal equilibrium . The data must be corrected for the dilution heats associated with the addition of buffer into tRNA and complex **1** into buffer solution. The area under each peak was integrated, heats of dilution are subtracted and the thermogram for the binding of complex **1** to tRNA has been obtained (Fig. 4). The heat released during the binding is related to enthalpy (ΔH) and entropy (TΔS), free energy (ΔG), number of binding sites (n) and binding affinity (K_b). These thermodynamics parameters are related to each other by the following equations [19]:

$$\Delta G = \Delta H - T\Delta S \qquad (3)$$

$$\Delta G = -RT \ln K_b \qquad (4)$$

According to Eqs. (3) and (4), we calculated ΔH = –97.97 kJ.mole^{-1}, ΔG = –26.54 kJ.mole^{-1}, ΔS = +239.69, n = 1.11 and K_b = 4.504 ×10^4 M^{-1}. The results indicated that the binding of complex **1** to tRNA is driven by favorable enthalpy along with unfavorable entropy contributions and complex **1** bound to tRNA through groove binding and clearly rule out the intercalative binding of the complex to tRNA. Additionally, the apparent enthalpy increase accompanied a variety of non–covalent molecular interactions, such as specific hydrogen bonds, hydrophobic interactions and van der Waals force [20]. The negative ΔH and positive ΔS values suggest that hydrophobic and hydrogen bond interactions play major roles in the complex **1**– tRNA binding reaction and contributed to the stability of the complex.

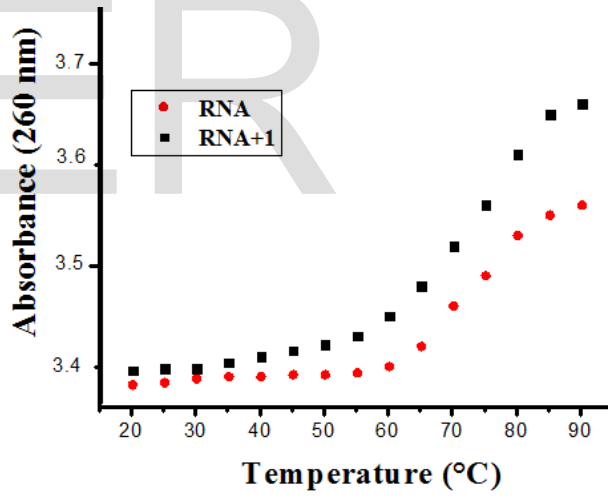

Fig.5. Thermal melting curves of tRNA (●), tRNA + complex **1** (■). (For interpretation of the references to color in this figure legend, the reader is referred to the web version of this article).

3.4 Thermal denaturation study

The ability of binding complex **1** to enhance the stability of the double–stranded tRNA is generally studied through optical melting studies. When tRNA is heated slowly, the double–stranded tRNA gradually dissociates to single–stranded tRNA, which generates a hyperchromic effect on the absorption spectra (λ_{max}= 260 nm) of single–stranded tRNA is much higher than in double–stranded tRNA [21]. In general, electrostatic binding along the phosphate backbone of tRNA gives rise to only a small change (3–6 °C) in thermal denaturation

temperature, while intercalation leads to a significant rise in thermal denaturation temperature of tRNA due to the stabilization of the Watson–Crick base–paired duplex. Therefore, thermal denaturation experiment of tRNA provides a convenient tool for detecting binding and also assessing relative binding strengths [22]. In the present work, the melting curves of tRNA in the absence and the presence of complexes **1** is presented in Fig. 5. The ΔT_m values of tRNA in the presence of complex **1** is 6 °C, which is characteristic of non–intercalative binding behavior [23].

3.5 Resonance energy transfer across the tRNA.

Fluorescence resonance energy transfer (FRET) is a quantum phenomenon that can be occurs *via* overlapping of emission spectrum of a fluorophore (donor) overlaps with the absorption spectrum of another molecule (acceptor) based on the degree of transition dipole coupling. This process only occurs when the donor and acceptor molecules are sufficiently close to each other, i.e. at a distance of 10–100 Å according to Förster's theory [24]. For each fluorescence platform, an appropriate dye or combination of dyes had to be selected.
EB is known to intercalate into tRNA. Upon intercalation, EB's fluorescence is greatly enhanced. It has been determined that approximately ten molecules of EB are bound to a single tRNA molecule, yet only three molecules of EB are bound in sites that facilitate EB fluorescence.53 A single strong EB binding site is located adjacent to the sixth base pair of the acceptor stem in tRNA [25]. For use EB as intercalator binding agent into tRNA transferred to complex **1** *via* a Förster type resonance energy transfer when complex **1** simultaneously bound to tRNA.

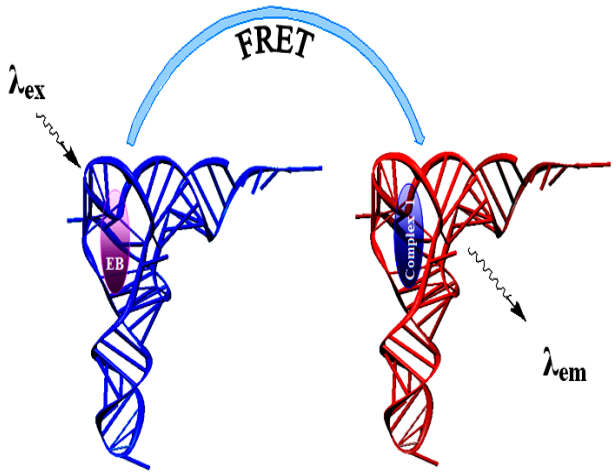

Fig.6. Fluorescence resonance energy transfer (FRET) mechanism.

Under adequate experimental conditions (concentration and distance), the fluorescence observed when using the excitation wavelength of the donor corresponds to the acceptor because the emission energy of the donor is transferred to the acceptor (Fig. 6). According to FÖster resonance energy transfer (FRET), the efficiency of energy transfer €, as follows, is obeyed according to Foster's theory [26]:

$$E = 1 - \frac{F}{F_0} = \frac{R_0^{\,6}}{r^6 + R_0^{\,6}} \qquad (5)$$

$$r_{DA}^6 = \frac{[R_0^6(1-E)]}{E} \qquad (6)$$

where F and F_0 are the fluorescence intensities of EB– tRNA in the presence and absence of acceptor (complex **1**), *r* is the distance between acceptor and donor, and R_0 is the critical distance when the transfer efficiency is 50%. The value of R_0 was calculated using the Eq. (7):

$$R_o = 9.78\times10^3\left(\kappa^2 n^{-4} Q_D J(\lambda)\right)^{1/6} \text{ (in Å)} \qquad (7)$$

where κ^2 is the spatial factor of orientation (= 2/3), n is refractive index of the medium (= 1.33), Q_D is the fluorescence quantum yield of the donor (= 0.78), and $J(\lambda)$ is the overlap integral between donor emission and acceptor absorption defined as:

$$J(\lambda) = \frac{\int_0^\infty F_D(\lambda)\varepsilon(\lambda)\lambda^4\Delta\lambda}{\int_0^\infty F_D(\lambda)\Delta\lambda} \qquad (8)$$

Here $F_D(\lambda)$ is the fluorescence of the donor in the wave length range λ and λ +d λ, and $\varepsilon(\lambda)$ is the molar extinction coefficient of the acceptor at the wavelength λ. The overlap of the absorption spectrum of the complex **1** with the fluorescence emission spectra of EB– tRNA system is shown in Fig. 7.

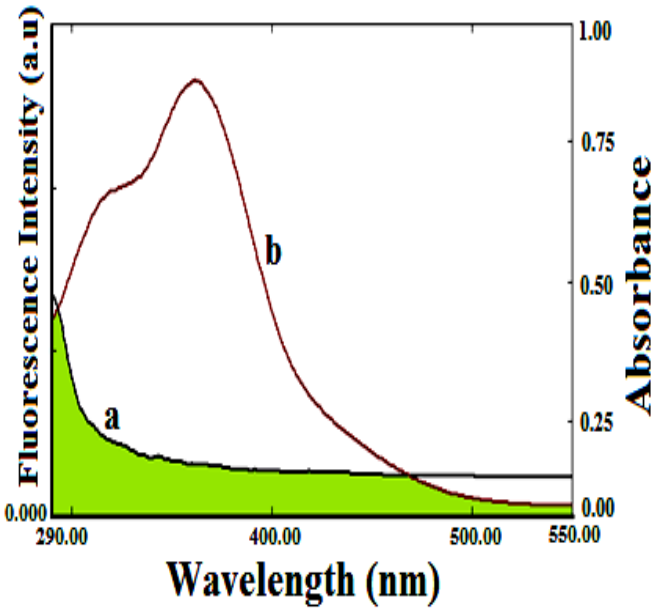

Fig.7. Overlap of UV absorption spectra of complex **1** (a) with the fluorescence emission spectra of tRNA (b). The fluorescence emission spectrum of tRNA (1.0×10^{-5} M) and the UV absorption spectrum of complex **1**

(1.0×10^{-5} M).

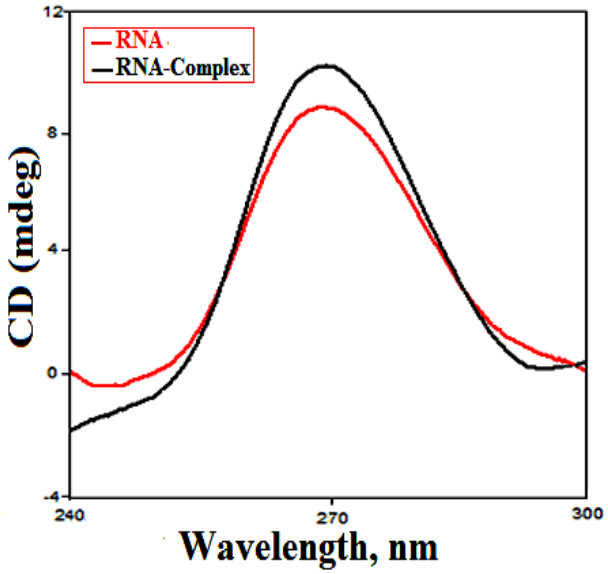

Fig. 8. CD spectra of (A) tRNA alone (B) tRNA in the presence of complex **1** in 5 mM Tris– HCl/50 mM NaCl buffer at 25 °C. [Complex] 1.0×10^{-4} M, [tRNA] 1.0×10^{-4} M.

The efficiency of energy transfer is calculated by using eq 4b and found to be 97 %. The estimated donor (complex **1**)–acceptor (tRNA) distance (*r*), utilizing eq 1, is found to be 37 Å (at 25°C). The observation indicates simultaneous binding of the complex **1** to the tRNA at room temperature.

3.6 Circular dichroism studies

Circular dichroism (CD) is a powerful and sophisticated tool for identifying conformational changes of tRNA. The observed CD spectrum of tRNA consists of a large positive band at ~ 270 nm due to base stacking interactions, and a weak negative band at ~ 238 nm due to backbone interactions, In general, electrostatic interaction of the complexes with tRNA showed less or no perturbations on the base stacking and helicity bands while intercalator enhances the intensities of both the bands. On incubation of present complex **1** with tRNA, the CD spectrum of tRNA undergoes changes in both positive and negative bands (Fig.8). In complex **1**, after addition of tRNA the CD spectrum shows decrease in positive and in negative bands without shift in the band position. Such results suggest that the CD spectra are closely correlated with tRNA binding affinity [27].

3.7 Cell viability

The synthetic water soluble complexes were also screened for their anticancer activities as SW480 cell line was the target. The cancer cells were incubated in the presence of increasing concentration of the complexes for 24 h, and the anti–proliferation activity was measured according to the procedure described in the experimental part [28]. As shown in Fig. 9. Complex **1** exhibits significant inhibitory effects against the cancer cell line at the range of 0.0 –20 µg/ml. The IC_{50} value of complex **1** is 2.78 µg/ml, which is defined as the concentration of a compound where 50% of the cell growth is inhibited. These results revealed that complex **1** acts as a potential selective anticancer agent with significant GI_{50} values specifically towards SW480 tumor cell line.

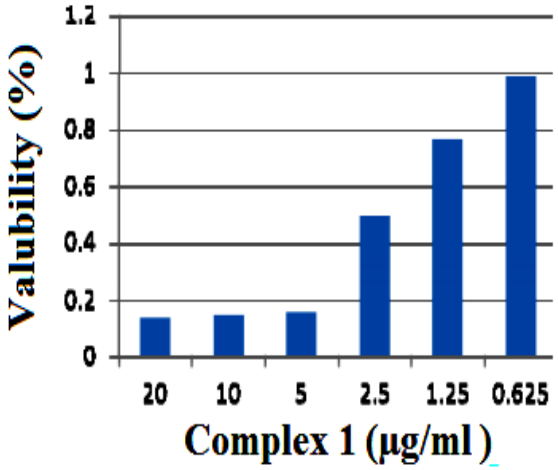

Fig.9. Growth inhibition on SW480 cells.

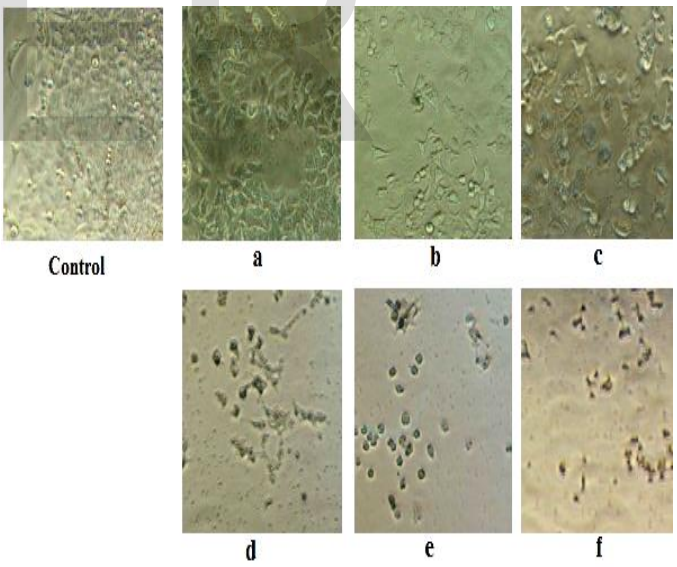

Fig.10. Inverted microscopic images of SW480 cells incubated separately with only the culture medium as the control (a), 0.625 µM/ml complex **1** (b), 1.25 µM/ml complex **1** (c), 5 µM/ml complex **1** (d), 10 µM/ml complex **1** (e), 20 µM/ml complex **1** (f) for 24 h.

3.8 Optical microscopic inspection

The optical microscopic images of cells were displayed in Fig.10. Obviously, the SW480 cancer cells appeared spindle–shaped cell (Fig.10a). A large number of cells induces changes in cell shape and morphology and the adherence cell number decreased. The density of cells was evidently decreased with

the treatment of 0.625 –20 μg/ml complex **1** (Fig.10b–f), Furthermore, when the cancer cells were treated with high concentration of complex **1** (20 μg/ml), most of the cells were gathered together and suspended in the culture medium. These results indicated that complex **1** could induce the change of cell morphology and inhibit the cancer cells growth in a dose–dependent manner.

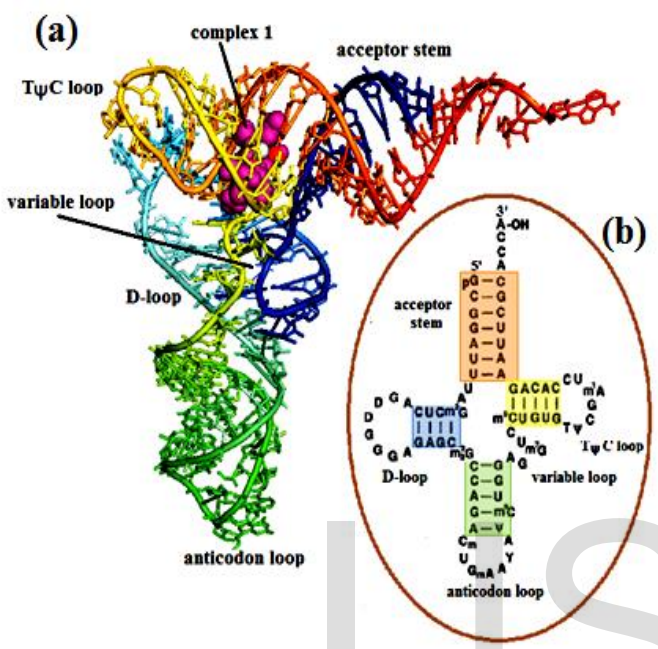

Fig.11. (a) Docking structure between complex **1** and yeast tRNA (PDB ID: 1EHZ) and (b) cloverleaf model structure of tRNA.

3.9 Molecular docking with tRNA

tRNAs are versatile molecules with cloverleaf structure that show high degree of folding stabilized by base stacking, base pairing and other tertiary interactions. In order to get more insight into the mode of binding, complex **1** was successively docked with tRNA to determine the preferred binding sites on tRNA. The most extensive region calculated as a binding site for positively charged probes in both tRNAs is located in the deep groove near the junction of the anticodon stem and D stem where, in the crystal structure of $tRNA^{Phe}$ [29]. $t–RNA^{phe}$ (Fig.11) is one of the most thoroughly characterized naturally occurring RNA molecule available for such interaction study. In our experiment, rigid molecular docking studies was performed to predict the binding modes of complex **1** with a tRNA (PDB ID : 1EHZ), and provide an energetically favorable docked pose that is shown in Fig.12. complex **1** is in the vicinity of C–49, U–50, G–51, U–59, C–63, and A–64 with the free binding energy of –25.74 kcal/mol. The extra stability is related to the presence of H–bonding between N3 of guanine–51 and the NH of piperazine and O2 of U59A with amino functionality of dipeptide (glygly) in complex **1**. The results between complex **1** and tRNA were appropriate well with the spectroscopic binding studies.

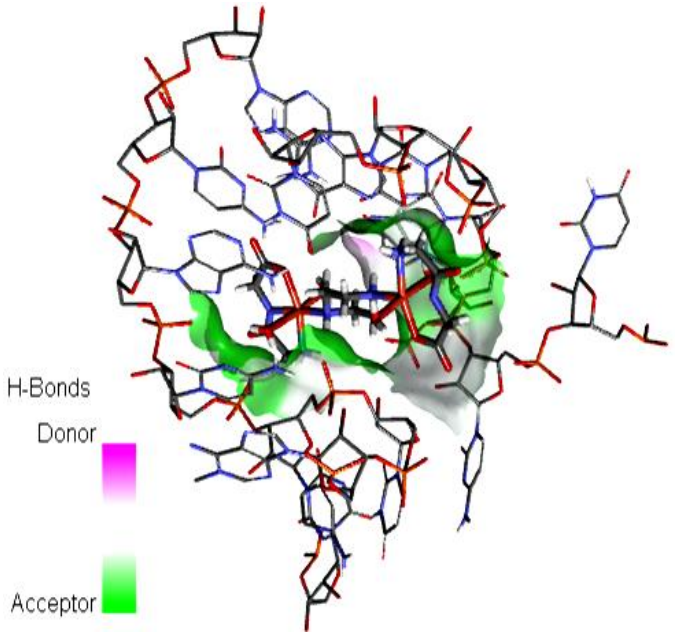

Fig.12. The interaction mode between complex 1 with tRNA. (green colour surface showing hydrogen bond interaction between them.).

4 Conclusion

In this work, we have explored the interaction studies of a new dinuclear copper(II) complex derived from the dipeptide (glycylglycine) and piperazine as a metallopeptide drug to examine their effect on the binding propensity of tRNA and to elucidate the mechanism of action at the molecular target. The interaction of tRNA with complex **1** was investigated by employing different spectroscopic techniques in accordance with molecular docking techniques. The *in vitro* DNA binding studies of complex **1**reveal an electrostatic binding mode. The results of optical microscopic inspection and MTT assay showed that the complex **1** (0.625 –20 μg/ml) could reduce the viability of SW480 cells in a dose-dependent manner. The distance between donor (tRNA) and acceptor (complex **1**) was obtained according to fluorescence resonance energy transfer (FRET). Additionally, molecular docking studies were performed with molecular target tRNA and in order to validate the experimental results. Therefore, it is concluded that drugs that bind to the tRNA (acceptor stem site) represent an important class of anticancer drugs.

Acknowledgements

Author WMA thanks Ministry of Higher Education & scientific Research, Sana'a, Yemen (Ser. no. 01139/2009) for

the sanction of major research grant. Also author ST thanks University Grants Commission, New Delhi for financial support through research grant No. F31–100/2005(SR). Authors are thankful to Dr. Rizwan Hasan Khan for performing ITC and CD studies.

REFERENCES

[1] Yakuphanoglu F, Sekerci M (2005)Determination of the optical constants of Co(II) complex of Schiff base obtained from 1,8-diaminophthalene thin film by infrared spectra. Journal of Molecular Structure 751: 200–203.)

[2] Marzano C, Pellei M, Tisato F, Santini C (2009) Copper complexes as *anticancer agents*.. Anti–Cancer Agent Med Chem 9: 185–211.

[3] Chen D, Cindy QC, Yang H, Dou QP (2006) Disulfiram, a Clinically Used Anti–Alcoholism Drug and Copper–Binding Agent, Induces Apoptotic Cell Death in Breast Cancer Cultures and Xenografts via Inhibition of the Proteasome Activity. Cancer Res 66(21): 10425–10433.

[4] Foloppe N, Matassova N, Aboul–ela F (2006) Towards the discovery of drug–like RNA ligands?. Drug Discovery Today 11 (21/22): 1019–1027.

[5] Nelson P, Kiriakidou M, Sharma A, Maniataki E, Mourelatos Z (2003) The micro RNA world: Small is mighty. Trends Biochem Sci 28: 534–540.

[6] Gallego J, Varani G (2001) Targeting RNA with small–molecule drugs: therapeutic opportunities and chemical challenges. Acc Chem Res 34: 836–843.

[7] Corey DR (2007) Chemical modification: the key to clinical application of RNA interference. J. Clin. Invest.117: 3615–3622.

[8] Paul P, Kumar GS (2013) Targeting ribonucleic acids by toxic small molecules: Structural perturbation and energetics of interaction of phenothiazinium dyes thionine and toluidine blue O to $tRNA^{phe}$. J Hazard Mater 263: 735–745.

[9] Tabassum S, Al–Asbahy WM, Afzal M, Arjmand F, Bagchi V (2012) Molecular drug design, synthesis and structure elucidation of a new specific target peptide based metallo drug for cancer chemotherapy as topoisomerase I inhibitor. Dalton Trans 41: 4955–4964.

[10] Islam MM, Sinha R, Kumar GS (2007) RNA binding small molecules: studies on t–RNA binding by cytotoxic plant alkaloids berberine, palmatine and the comparison to ethidium. Biophys Chem, 125: 508–520.

[11] Reicmann ME,. Rice SA, Thomas CA, Doty P (1954) A Further Examination of the Molecular Weight and Size of Desoxypentose Nucleic Acid**.** J Am Chem Soc 76: 3047–3053.

[12] Wolfe A, Shimer GH, Meehan T (1987) Polycyclic aromatic hydrocarbons physically intercalate into duplex regions of denatured DNA. Biochemistry 26: 6392 –6396.

[13] Mustard D, Ritchie DW (2005) Docking essential dynamics eigenstructures. Proteins: Struct Funct Bioinf 60: 269–274.

[14] Liang X, Zou X, Tana L, Zhu W, (2010) Study on nucleic acid (CT–DNA and yeast tRNA) binding behaviors and cytotoxic properties of a heterodinuclear Ru(II)–Co(III) polypyridyl complex. Journal of Inorganic Biochemistry104:1259–1266.

[15] Wilson WD, Ratmeyer L, Zhao M, Strekowski L, Boykin D (1993)The search for structure- specific nucleic acid- interactive drugs: Effects of compound structure on RNA versus DNA interaction strength. Biochemistry 32: 4098–4104.

[16] Luedtke NW, Hwang JS, Nava E, Gut D, Kol M, Tor Y, (2003) The DNA and RNA specificity of eilatin Ru(II) complexes as compared to eilatin and ethidium bromide. 31: 5732–5740.

[17] Lakowiez JR, Weber G (1973) Quenching of fluorescence by oxygen. Probe for structural fluctuations in macromolecules. Biochemistry 12: 4161–4170.

[18] Lo ATS, Salam NK, Hibbs DE (2011) Rutledge PJ, Todd MH, Polyamide–Scorpion Cyclam Lexitropsins Selectively Bind AT–Rich DNA Independently of the Nature of the Coordinated Metal. PLoS ONE 6: 17446–17446.

[19] Salim NN, Feig AL (2009) Isothermal titration Calorimetry of RNA. Methods 47: 198–205.

[20] Pierce MM, Raman CS, Nall BT (1999) Isothermal Titration Calorimetry of Protein–Protein Interactions. Methods19: 213–221.

[21] Onori G, Santucci A (1996) Dynamical and structural properties of water/alcohol mixtures. Journal of Molecular Liquids 69: 161–181.

[22] Mei H–Y, Barton JK(1988) Tris(tetramethylphenanthroline) ruthenium(II): a chiral probe that cleaves A–DNA conformations. Proc. Natl. Acad. Sci. U.S.A 85(5): 1339–1343.

[23] Giri P, Kumar SG (2007) Specific binding and self structure induction to poly(A) by the cytotoxic plant alkaloid sanguinarine. Biochim Biophys Acta 1770: 1419–1426.

[24] Nomanbhoy TK, Schimmel P (2001) Active Site of an Aminoacyl–tRNA Synthetase Dissected by Energy–Transfer–Dependent Fluorescence. Bioorganic & Medicinal Chemistry Letters 11: 1485–1491.

[25] Xu H, Deng H Zhang, Q–L, Huang Y, Liu J–Z, Ji L–N (2003) Synthesis and spectroscopic RNA binding studies of $[Ru(phen)_2MHPIP]^{+2}$. Inorganic Chemistry Communications 6: 766–768.

[26] Lakowicz JR, (1999) Principles of Flourescence Spectroscopy. Kluwer Academic/Plenum Publishers 2nd ed: New York.

[27] Islam MM, Pandya P, Chowdhury SR, Kumar S, Kumar GS (2008) Binding of DNA binding alkaloids berberine and palmatine to tRNA and comparison to ethidium: Spectroscopic and molecular modeling studies. Journal of Molecular Structure 891:498-507.

[28] Maree C. Faux, Janine L. Ross, Clare Meeker, Terry Johns, Hong Ji, Richard J. Simpson, Meredith J. Layton and Antony W. Burgess (2003) Restoration of full–length adenomatous polyposis coli (APC) protein in a colon cancer cell line enhances cell adhesion. Journal of Cell Science 117: 427–439.

[29] Agudelo D, Bourassa P, Beauregard M, Bérubé G, Tajmir–Riahi H–A (2013) tRNA Binding to Antitumor Drug Doxorubicin and Its Analogue. PLOS ONE 8: e69248– e69248.